Computer-AidedDesign

Taylor & Francis
Taylor & Francis Group

Generating a reference model of the surface with a hole for downstream process

Gulibaha Silayi[1] , Tsutomu Kinoshita[2] , Katsutsugu Matsuyama[1] and Kouichi Konno[1]

[1]Iwate University, Japan; [2]Fukui University of Technology, Japan

ABSTRACT

The value of 3D CAD models is continuously increasing in downstream processes. The more extensive use of a 3D model outside traditional design and manufacturing is trending now. To distribute 3D data quickly to downstream departments is significant boosts to product quality, production costs, and delivery to markets. Unfortunately, interoperability causes poor communication since downstream applications rely on the reusability and interoperability of CAD models. However, 3D CAD data size for expressing precise forms tends to be big and time-consuming for computation, which may interfere in the communication. In addition, downstream processes emphasize surface smoothness more than precision. Therefore, this paper describes the reconstruction method of a smooth surface by integrating the advantages of Gregory and B-spline surfaces. In this paper, a new surface representation is proposed. Two surfaces are connected with G^1-continuity by using the control points at the common boundary obtained from joining equations. The internal control point that is not connected to the boundary curve is obtained from the least squares approximation method. The proposed method is applicable to shapes with a hole.

1. Introduction

3D data designed with 3D CAD systems are becoming vital communication tools between the design process and downstream processes. Quickly distributing 3D data to downstream departments can dramatically enhance their work efficiency. In the downstream department, 3D data received from a design department can be effectively utilized as a reference model for the creation of various process procedures and technical documents, such as creating visual assembly instructions, creating product manuals and product catalogs. In such works, clear visual communication for ease of understanding is important. However, size of 3D CAD data for expressing precise forms tends to be big and takes long time to compute, therefore it may interfere with communication among users. In addition, since the internal data structures and tolerances do not coincide in each system, the intended shape model for downstream distribution may not be delivered correctly. If the shape delivery fails in one system, the shape should be modified through some method to import suitably within the system. To overcome the problem, the direct modeling which modifies the curve mesh is effective. For example, Fig. 1 shows the gap between two trimmed surfaces which was caused by the different tolerances. The gap is one of the most serious interoperability challenges between CAD, CAM and CAE systems [2]. In direct modeling, modification of a trimmed surface [1] has the restriction where boundary edges must lie on the surface within a certain tolerance. Thus, it is difficult to maintain geometrical consistency of the modified boundary edges and surfaces. Therefore, it is effective to apply a new free-form surface to a closed region enclosed with modified boundary edges because the consistency of the trimmed surface can be maintained. Since downstream processes concern surface smoothness rather than the precision of the approximated surface, the smoothness is more important than the approximation precision. Because, 3D surface models show the entire 3D image and shape of an object, so the visual impact is more important. For instance, Fig. 2 illustrates the importance of the visible connections between surfaces of two same 3D objects. At a first glance, we can see that which one is more appropriate as a reference model. In consideration of the discontinuity at connection parts as marked in red circles in Fig. 2(b), Fig. 2(a) is more appropriate than Fig. 2(b) as a reference model. The problem of smooth connection will reduce the quality of the data as a reference model. In conventional surface fitting method which approximates a surface using sample points derived from the tangent plane, the continuity with an adjacent surface will collapse because the surface was generated individually. In contrast, the surface fitting

CONTACT Gulibaha Silayi ✉ gulbahar@lk.cis.iwate-u.ac.jp
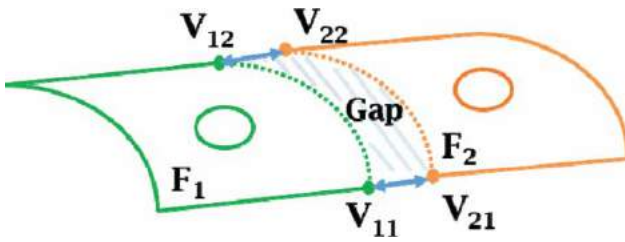
Figure 1. Modifying a boundary edge in direct modeling for data healing.
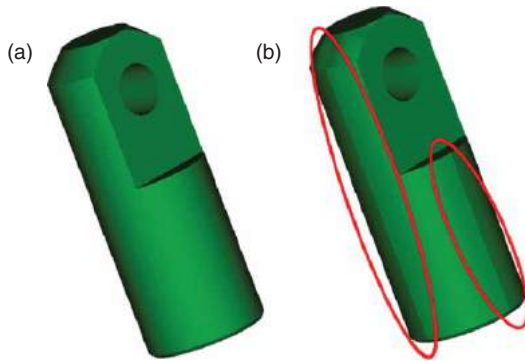

Figure 2. Example of surface smoothness.

method [5] is proposed by Muraki et al. in consideration of maintaining G^1-continuity with adjacent surfaces. In their method, G^1- continuity is guaranteed on the common boundary edges. However, when a surface connects with adjacent surfaces with G^1-continuity in two adjoining directions along the common boundary edges as shown in 3, the conditions used as G^1-continuous cannot be fulfilled near the corner portions with a B-spline surface. In Fig. 3(a), the red x marks are indicate the discontinuous portion near the corner of the common boundary edges.

The goal of this work is to propose a new surface representation to solve the problems of the Muraki's method.

In this method shapes can be approximated in good accuracy as a reference model for downstream processes. Our method generates a trimmed surface that is G^1-continuous with adjacent surfaces in all directions and applicable to shapes with a hole.

2. Related work

In the field of CAD, construction of N-side region has received a lot of attention. Muraki et al. proposed a reconstruction method of trimmed surfaces for an N-side region and allowed discontinuous portions near the corners of the common boundary edges [5]. His method unites the advantages of the surface interpolation method [4,11] and the N-side filling method [5]. On a common boundary where two surfaces should be connected with G^1-continuity, an input curve mesh is represented by cubic Bezier curves and the cross boundary derivatives are calculated based on the basis patch method [7]. Among control points of the B-spline surface, the control points lying on the inner side of the boundary curves are calculated by the surface interpolation method. Moreover, other internal control points are calculated by the N-side Filling method. However, by using conventional B-spline surfaces, the cross-boundary derivative vectors cannot be specified independently. Concretely, as shown in Fig. 3(b), the control point 'A' indicates the only control point that involves in calculation of a B-spline surface cross-boundary derivatives in u and v directions. Therefore, when the connection with adjacent surfaces performed successively in u and v directions, B-spline has no degree of freedom to individually define the connections of two surfaces with G^1-continuity in u and v directions. Moreover, when a surface connects with adjacent surfaces in two adjoining directions along common boundary edges as shown in Fig. 3(a), knots are inserted near the corners (at parameters 0.05 and 0.95) [5] in order to narrow down the discontinuous section with the adjacent
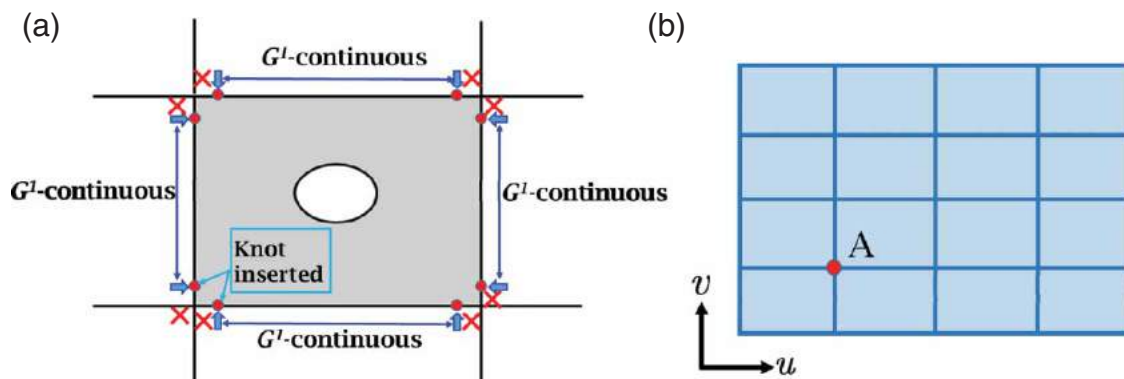
Figure 3. Problems of the method of Muraki et al. [5].

surfaces even if two surfaces have to be connected with G^1-continuity. However, the method of determining the knot values near the corners are unclear.

In surface reconstruction, how to guarantee a smooth connection between adjacent B-spline surfaces, is very important. Mu et al. proposed the construction of B-spline surfaces by interpolating its boundary curves, or even the cross-boundary derivatives, and the inner points were approximated simultaneously [8]. In their method, a B-spline surface is smoothly connected with adjacent surfaces, however, it cannot be respond to local modification and the applicability to the shapes with a hole was not discussed in the literature.

In this paper, we mainly focus on the problems of Muraki et al. and propose a new surface representation with which the cross-boundary derivatives can be specified independently in both u and v directions with the B-spline blending functions.

3. New surface representation

This research integrates the advantages of the B-spline and Gregory surfaces to define a new surface representation. To be more concrete, construction of a new surface representation via the boundary curves and approximation of the inner control points will be studied. We express a fitting surface $S(u, v)$ using surface control points $P_{i,j,k}(i = 0, \ldots, n; j = 0, \ldots, m; k = 0, 1)$. Surface $S(u, v)$ is expressed by Eqn. (3.1), where $N_i^3(u)$ and $N_j^3(v)$ are the cubic B-spline basis functions over the knot spans

$$U = \begin{bmatrix} 0, & 0, & 0, & 0, & u_0, & \ldots, & u_p, & 1, & 1, & 1, & 1 \end{bmatrix} \quad \text{and}$$
$$V = \begin{bmatrix} 0, & 0, & 0, & 0, & v_0, & \ldots, & v_q, & 1, & 1, & 1, & 1 \end{bmatrix}.$$

$$S(u, v) = \sum_{i=0}^{n} \sum_{j=0}^{m} N_i^3(u) N_j^3(v) Q_{i,j}(u, v) \quad (3.1)$$

The rational functions $Q_{i,j}(u, v)(0 \le i \le n; 0 \le j \le m)$ are defined by the following relationships:

1. If $(i, j) = (1, 1), (1, m - 1), (n - 1, 1), (n - 1, m - 1)$, then

$$Q_{1,1}(u, v) = \frac{uP_{110} + vP_{111}}{u + v}$$
$$(0 < u < u_0, 0 < v < v_0) \quad (3.2)$$

$$Q_{1,m-1}(u, v) = \frac{uP_{1(m-1)0} + (1 - v)P_{1(m-1)1}}{u + (1 - v)}$$
$$(0 < u < u_0, v_q < v < 1) \quad (3.3)$$

$$Q_{n-1,1}(u, v) = \frac{(1 - u)P_{(n-1)10} + vP_{(n-1)11}}{(1 - u) + v}$$
$$(u_p < u < 1, 0 < v < v_0) \quad (3.4)$$

$$Q_{n-1,m-1}(u, v) = \frac{(1 - u)P_{(n-1)(m-1)0} + (1 - v)P_{(n-1)(m-1)1}}{(1 - u) + (1 - v)}$$
$$(u_p < u < 1, v_q < v < 1) \quad (3.5)$$

2. If others, then

$$Q_{i,j} = P_{ij0} \quad (3.6)$$

In our method, a surface is fitted using the Eqn. (3.1), and the concept of our method is shown in Fig. 4. Fig. 4(a) shows surface F that has G^1-continuous adjacent surfaces F_1, F_2, F_3 and F_4 in all four directions. On a common boundary where two surfaces are connected with G^1-continuity, each boundary of an input curve mesh is represented by a cubic Bezier curve. The concept of our proposed method explains in the case where knots are inserted at parameters $u_0 = 0.5$ and $v_0 = 0.5$ ($p = 0, q = 0$) as shown in Fig. 4(b). The yellow control points are obtained from boundary curves, the red ones are obtained by the joining equations [3] and the blue one is obtained by the least squares approximation method.
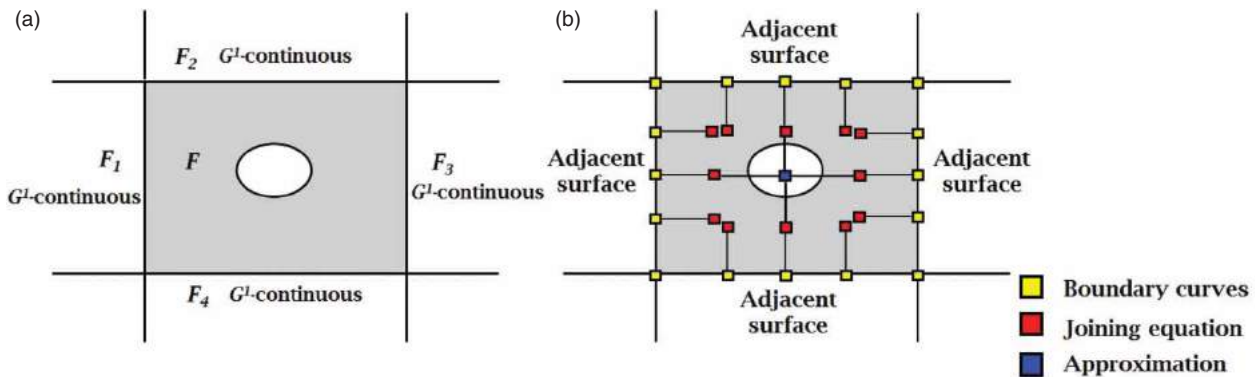

Figure 4. Concept of our proposed method (b) applied to the gray region of (a).

First, when two surfaces are connected with G^1-continuity, we calculate the G^1-continuous control points at the common boundary by using joining equations described in section 3.1. Next, a bi-cubic Gregory patch is constructed by the G^1-continuous control points. Since the constructed Gregory patch is insufficient for representing a trimmed surface, knots are inserted in both u and v directions for increasing the degree of freedom. Then, the unknown inner control points are optimized using least squares approximation method [9]. Finally, a new surface is constructed using Eqn. (3.1).

3.1. Joining with the adjacent surface

In order for two surfaces S^1 and S^2, with a common boundary curve shown in Fig. 5(a) to have a G^1-continuity, the derivative vectors on the boundary curves should satisfy the condition defined by Eqn. (3.7) [3], where $k(v)$ and $h(v)$ are scalar functions of v as shown in Eqn. (3.8) [3]. If the vectors are set to $a_i(i = 0, \ldots, 3)$, $b_i(i = 0, \ldots, 3)$, $c_i(i = 0, \ldots, 2)$ as shown in Fig. 5(b). The G^1-continuous control points are calculated by solving Eqn. (3.9) and (3.10) (see APPENDIX for the derivation), where k_0, k_1 are positive real numbers and h_0, h_1 are arbitrary real numbers. To be more concrete, the cross boundary derivatives of the two surfaces are calculated by the joining equations [3], and control points which G^1-continuous with adjacent surfaces are obtained. The obtained cross boundary derivatives serve as a condition for connecting two surfaces with G^1-continuity.

$$\frac{\partial S^2(0, v)}{\partial u} = k(v)\frac{\partial S^1(1, v)}{\partial u} + h(v)\frac{\partial S^1(1, v)}{\partial v} \quad (3.7)$$
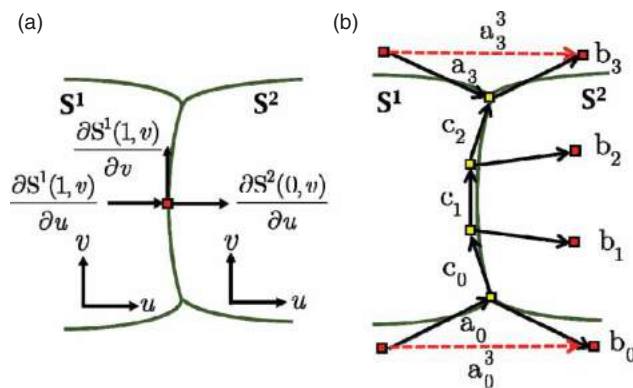
$$k(v) = k_0(1 - v) + k_1 v,$$

Figure 5. (a) G^1-continuity condition and (b) connection of two surfaces using the joining equations [3].

$$h(v) = h_0(1 - v) + h_1 v. \quad (3.8)$$

$$a_0^3 = \frac{a_0 + b_0}{|a_0 + b_0|}, \quad a_3^3 = \frac{a_3 + b_3}{|a_3 + b_3|},$$

$$a_1^3 = \frac{2a_0^3 + a_3^3}{3}, \quad a_2^3 = \frac{a_0^3 + 2a_3^3}{3},$$

$$b_0 = k_0 a_0 + h_0 c_0, \quad (3.9)$$

$$b_3 = k_1 a_3 + h_1 c_2, b_1 = \frac{(k_1 - k_0)a_0^3}{3} + k_0 a_1^3$$

$$+ \frac{2h_0 c_1}{3} + \frac{h_1 c_0}{3}, b_2 = k_1 a_2^3$$

$$- \frac{(k_1 - k_0)a_3^3}{3} + \frac{h_0 c_2}{3} + \frac{2h_1 c_1}{3}. \quad (3.10)$$

4. Approximation

In this paper, the boundary information and sample points on the boundary edges which represent a hole are used to approximate the inner control point by the least squares approximation method. A new surface is constructed using the Eqn. (3.1).

4.1. Approximation process

In Fig. 6, our approximation process of the inner control point is shown. As our concept of proposed method explains, knots are inserted at parameters $u_0 = 0.5$ and $v_0 = 0.5$ ($p = 0$, $q = 0$). The process is executed in the following steps:

(1) The G^1-continuous control points are obtained from joining equations and bi-cubic Gregory patch is constructed. The vectors between control vertices $b_i, \tilde{b}_i(i = 0, \ldots, 3)$ are calculated for u direction. The vectors $d_j, \tilde{d}_j(j = 0, \ldots, 3)$ are calculated for v direction.
(2) Knots are inserted in both u and v directions. After knot insertion, vectors $r_i = u_0 b_i$, $(i = 0, \ldots, 4)$ are calculated and vectors $\tilde{r}_i, v_j, \tilde{v}_j$ are calculated in the same manner. Moreover, control points are obtained from scaled vectors $r_i, \tilde{r}_i$ and $v_i, \tilde{v}_j$ as shown in Fig. 6.
(3) The points on the boundary edges which represent a hole are calculated as sample points and the center point of the hole is also added to the sample points. It is better to add center point to the sample points because it will improve the approximation accuracy around the hole. In our method, each boundary edge which represent a hole is equally divided into 10 sections and the number of sample points $t = $ *the number of boundary edges which represent a hole* $\times$ 10 + 1 are assumed to be $A_s (0 \leq s \leq t)$. The
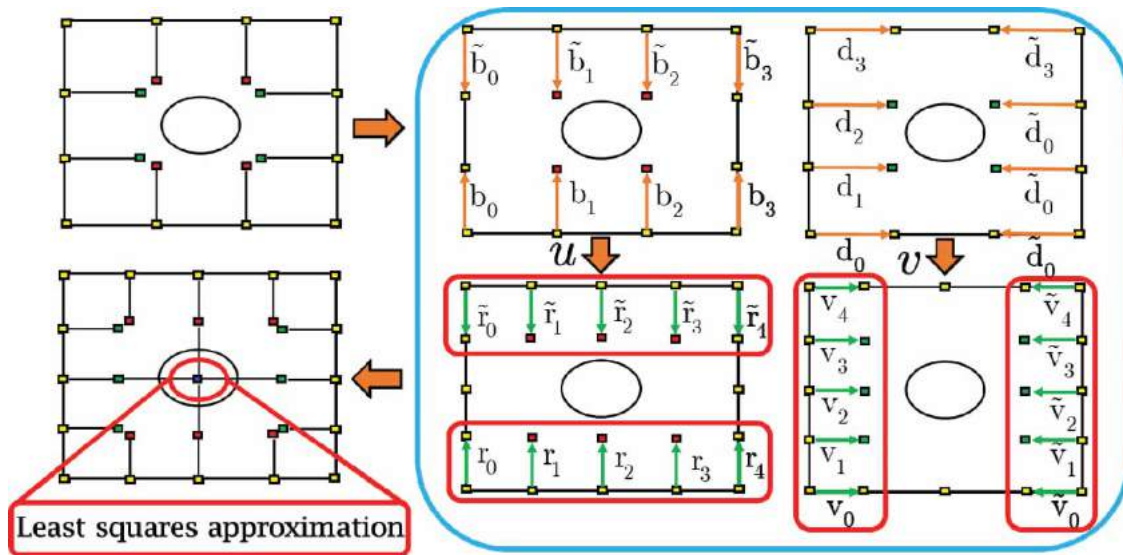
Figure 6. Inner control point approximation process.

parameters of A_s are assumed to be $\bar{u}_s$ and $\bar{v}_s$, and they are calculated by projecting A_s onto the Gregory patch constructed in step 1.

(4) From the control points generated in step 2 and the sample points generated in step 3, the unknown inner control point is approximated by using Eqn. (4.1).

(5) A new surface is constructed by the control points which were obtained in step 2 and the approximated inner control point which was obtained in

step 4.

$$f = \sum_{s=0}^{t-1} |A_s - S(\bar{u}_s, \ \bar{v}_s)|^2 \qquad (4.1)$$

4.2. Evaluation of generated surface

This section describes the evaluation method of the generated new surface. To verify the accuracy of the generated surface, the distance between the generated surface
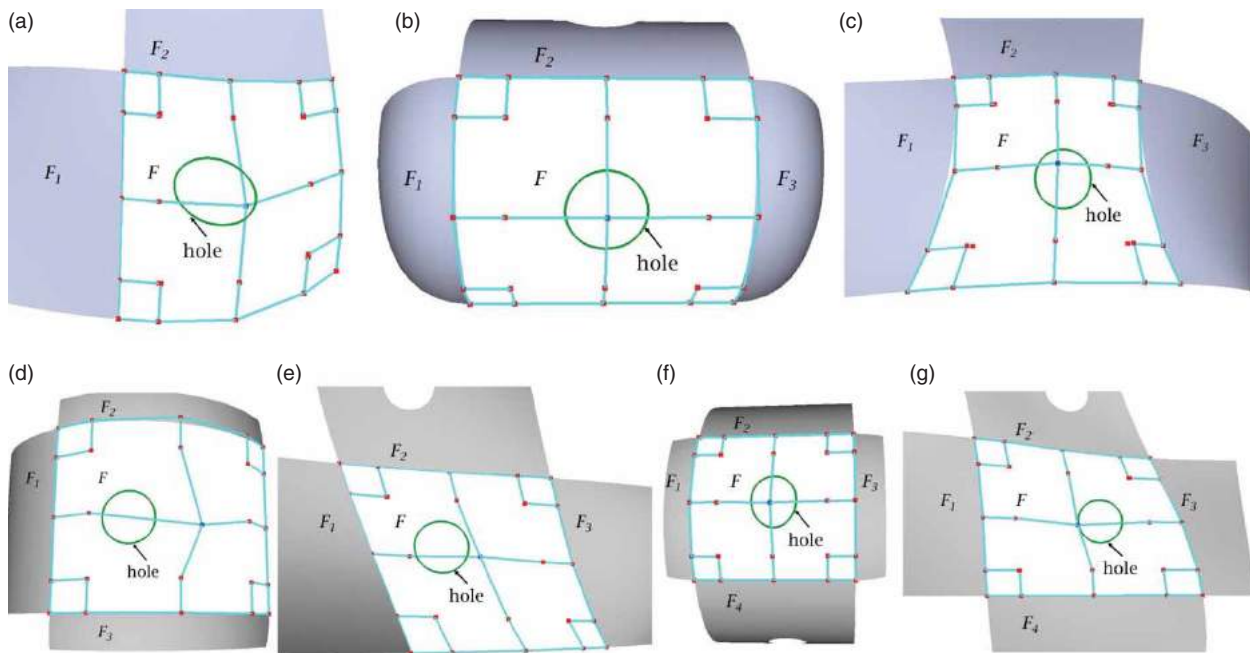

Figure 7. Control points of generated surfaces (a) to (g).

and the source surface retained by the trimmed surface is measured. The source surface was divided equally in both u and v directions into twenty sections so that a square grid was generated. The generated grid points on the source surface are projected to the generated surface and the distance between the source surface and generated surface is measured. Moreover, to find a relative error, the ratio of the bounding box size and the maximum distance are calculated [5]. In this paper, when ratio is smaller than 1% [5,10], it is assumed that a shape is approximated in good accuracy as a reference model for downstream processes.

5. Experimental results

Our method is applied to the shapes with a hole obtained from CAD data as shown in Fig. 6(a) to (g) and the practicality was verified. The generated surfaces were evaluated with the evaluation method described in section 4.2. Fig. 7(a) shows the control points of generated surface F that has G^1-continuous adjacent surfaces F_1 and F_2 in

two directions. Fig. 7(b) to (e) shows the control points of generated surface F that has G^1-continuous adjacent surfaces F_1, F_2 and F_3 in three directions. Fig. 7(f) and (g) shows the control points of generated surface F that has G^1-continuous adjacent surfaces F_1, F_2, F_3 and F_4 in all directions. The red dots indicate the control points generated in step 2 and the blue ones indicate the approximated control point in step 4, described in section 4.1.
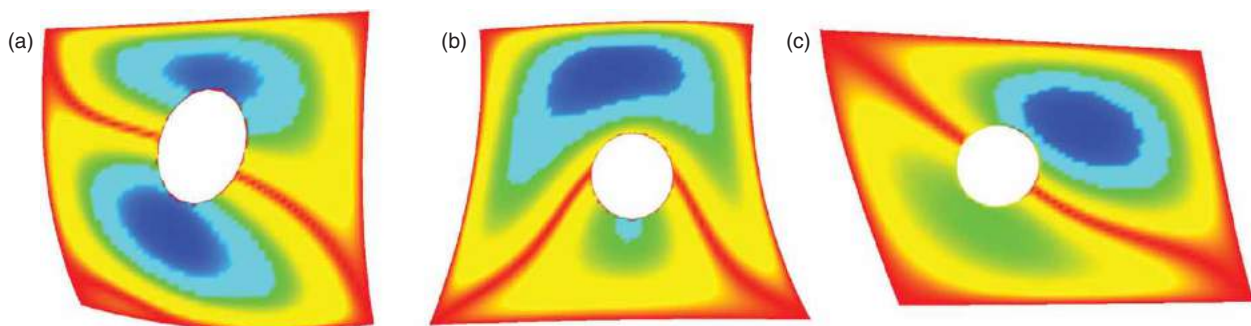
The error evaluation of the generated surface is shown in Tab. 1, *Avg.* indicates the average error margin value obtained by averaging the distances between the generated surface and the source one. *Max* indicates the maximum error margin value representing the maximum distance between the generated surface and the source one. *Ratio* indicates the ratio of the bounding box size and the maximum distance. The ratio of all objects (a) to (g) are less than 1% as shown in Tab. 1, and we can find that shapes are approximated in good accuracy as reference models for downstream processes. As described as the step. 3 in the section 4.1, it is better to add the center point to the sample points because it will improve the approximation accuracy around the hole. Tab. 2 shows the difference of error margins around the hole, obtained by adding the center point to the sample points. We can find that the approximation accuracy improved both on the average and maximum error margin values around the hole area by adding center point to the sample points. Additionally, the discrete evaluation result of a surface overall shape was visualized by generating a color map within a range of the distances between the generated

Table 1. Error evaluation.

Object	Evaluation object	Avg.	Max	Ratio
(a)	Trimmed surface	0.582885	1.865794	0.388339%
(b)	Trimmed surface	0.005640	0.024776	0.049194%
(c)	Trimmed surface	0.352679	1.139214	0.253059%
(d)	Trimmed surface	0.012622	0.068239	0.460547%
(e)	Trimmed surface	1.205581	4.220689	0.817447%
(f)	Trimmed surface	0.002428	0.011756	0.092034%
(g)	Trimmed surface	0.225614	0.895673	0.182698%

Table 2. Difference of error margins around the holes obtained by adding the center point to the sample points.

Data	With center point(Y) Avg.	Max	Without center point(N) Avg.	Max	Difference(Y-N) Avg.	Max
(a)	0.969301	1.578882	0.967025	1.589873	0.002276	−0.010991
(b)	0.026929	0.029018	0.063070	0.066205	−0.036141	−0.037187
(c)	0.284248	0.601748	0.303415	0.741213	−0.019167	−0.139465
(d)	0.009415	0.017530	0.009912	0.022806	−0.000497	−0.005276
(e)	0.706996	1.228102	0.750653	1.287324	−0.043657	−0.059222
(f)	0.010209	0.012188	0.011112	0.013014	−0.000903	−0.000826
(g)	0.243074	0.543374	0.248200	0.557874	−0.005126	−0.014500

Figure 8. Result of surface evaluation: distances between the generated surface and the source one are calculated. (a), (b) and (c) are the error margins of objects (a), (c) and (g) in Fig. 7 respectively.
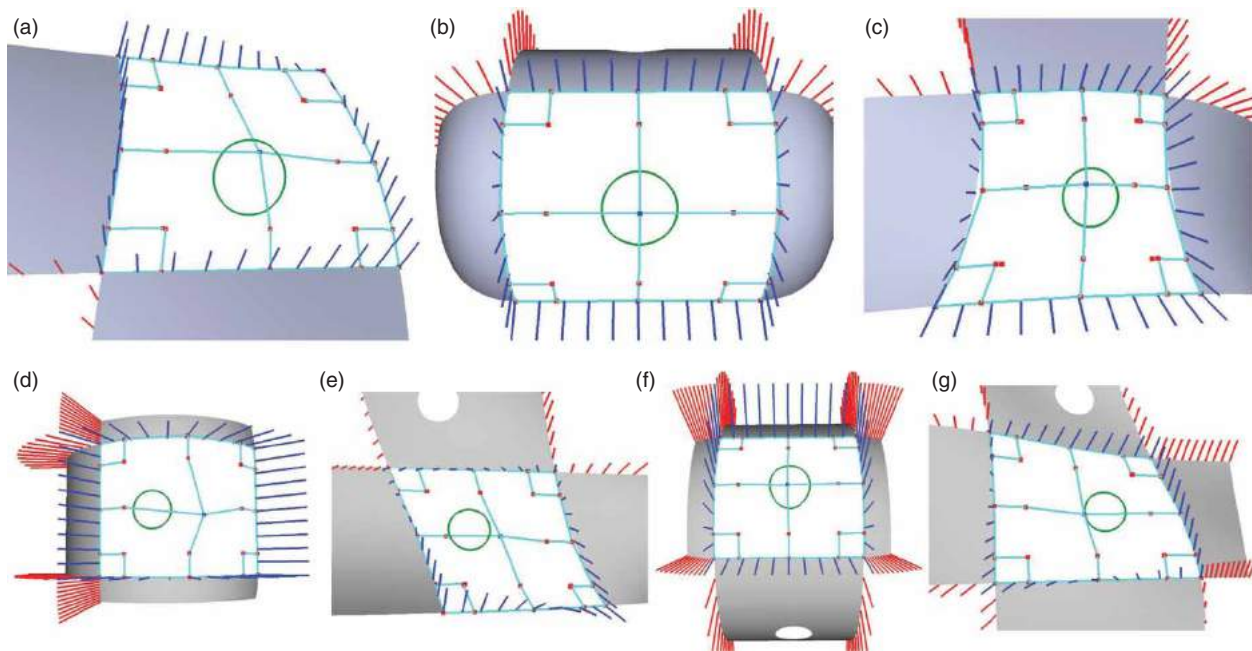
Figure 9. Verification of the continuity with adjacent surfaces: the normal vectors of the generated surfaces coincide with those of the adjacent surfaces on their boundary edges.

surface and the source surface as shown in Fig. 8(a) to (c). The red indicates the minimum error margins and the blue indicates the maximum error margins on the surface in Fig. 8.

Furthermore, in order to verify the continuity with adjacent surfaces, the normal vectors on the boundary edges of the generated surface are calculated, shown with blue lines in Fig. 9, and those of the adjacent surfaces are shown with red lines. As shown in Fig. 9 (a) to (g), the normal vectors of the generated surfaces coincide with those of the adjacent surfaces on their boundary edges, and we can find that two surfaces are connected with G^1-continuity.

6. Conclusion and future works

6.1. Conclusion

In this paper, we have proposed the method of generating a smooth surface with a hole that connects to adjacent surfaces with G^1-continuity by applying our new surface representation to a closed region. The proposed method integrates the advantages of the Gregory and B-spline surfaces. Concretely, the inner control points are obtained based on least squares approximation method, and the G^1-continuous control points on the boundary are obtained from the joining equations. Moreover, our method is independent of the position and the hole shape. Our method is also applicable to a region surrounded by surfaces in all directions connecting with G^1-continuity. Since our method generates a surface from boundary edge information, it is applicable to various applications. For instance, by including our method in the trimmed surface compression method [6,10] that the authors proposed, a smooth surface with good quality can be generated. It is also effective for direct modeling where shapes with a hole are modified.

6.2. Future works

In our method, by integrating the Gregory and B-spline surfaces, a smooth surface is generated in good accuracy for a downstream process as a reference model. Therefore, it is necessary to implement the new surface representation. In this paper, on a common boundary where two surfaces are connected with G^1-continuity, an input curve mesh is represented by cubic Bezier curves and the G^1-continuous control points on the boundary are obtained from the joining equations. Therefore, it is necessary to extend our method so that it can be applied to shapes with complex composite boundary curves or B-spline curves with multiple segments.

ORCID

Gulibaha Silayi 🆔 http://orcid.org/[0000-0002-4584-0906]
Tsutomu Kinoshita 🆔 http://orcid.org/[0000-0003-3836-2245]
Katsutsugu Matsuyama 🆔 http://orcid.org/[0000-0001-7476-9291]
Kouichi Konno 🆔 http://orcid.org/[0000-0002-1902-0939]

References

[1] Farin, G.: Curves and Surfaces for Computer Aided Geometric Design: A Practical Guide, fifth ed., San Diego, Academic Press, 2002.

[2] Kasik, D. J.; Buxton, W.; Ferguson, D. R.: Ten CAD model challenges, IEEE Computer Graphics and Applications, 25(2), 2005, 81–92. http://dx.doi.org/10.1109/MCG.2005.48

[3] Konno, K.; Chiyokura, H.: An Approach of Designing and Controlling Free-Form Surfaces by Using NURBS Boundary Gregory Patches, Computer Aided Geometric Design, 13(9), 1996, 825–849. http://dx.doi.org/10.1016/S0167-8396(96)00012-X

[4] Konno, K.; Tokuyama, Y.; Chiyokura, H.: A G^1 connection around complicated curve meshes using C^1 NURBS Boundary Gregory Patches, Computer Aided Design, 33(4), 2001, 293–306. http://dx.doi.org/10.1016/S0010-4485%2800%2900087-7

[5] Muraki, Y.; Matsuyama, K.; Konno, K.; Tokuyama, Y.: Reconstruction Method of Trimmed Surfaces with Maintaining G^1-continuity with Adjacent Surfaces, Computer-Aided Design and Applications, 11(2), 2014, 165–171. http://dx.doi.org/10.1080/16864360.2014.846085

[6] Muraki, Y.; Matsuyama, K.; Konno, K.; Tokuyama, Y.: Data Compression Method for Trimmed Surfaces Based on Surface Fitting with Maintaining G^1 Continuity with Adjacent Surfaces, Computer-Aided Design and Applications, 9(6), 2012, 811–824. http://dx.doi.org/10.3722/cadaps.2012.811-824

[7] Muraki, Y.; Matsuyama, K.; Konno, K.; Tokuyama, Y.: A Study of Surface fitting Method of an N-sided Region Considering G^1-Continuity with Adjacent Surfaces, in Proceedings of IWAIT 2012. (PDF:http://gmhost.lk.cis.iwate-u.ac.jp/member/49.pdf)

[8] Mu, G. W.; Zang, T.; Dai, S. J.: Surface Reconstruction via Interpolating Boundary Curves and Cross-Boundary Derivatives Simultaneously Approximating Inner Points, Applied Mechanics and Materials 321–324, 2013, 1821–1826. http://dx.doi.org/10.4028/www.scientific.net/AMM.321-324.1821

[9] Piegl, L.; Tiller, W.: The NURBS Book, Springer, New York, 1997, http://dx.doi.org/10.1007/978-3-642-59223-2.

[10] Silayi, G.; Kinoshita, T.; Muraki, Y.; Matsuyama, K.; Konno, K.: Evaluation of 3D Data Compression and Retrieval Method Based on Curve Mesh Filling, Computer Aided Design and Applications, 12(5), 2015, 1–9. http://dx.doi.org/10.1080/16864360.2015.1014732

[11] Toriya, H.; Chiyokura, H.: 3D CAD: Principles and Applications (Computer Science Workbench), Springer-Verlag, New York, Berlin, Tokyo, 1993. http://dx.doi.org/10.1007/978-3-642-45729-6

Appendix

In order for two surfaces S^1 and S^2, shown in Fig. 5(a) with a common boundary curve to have a G^1-continuity, the derivative vectors on the boundary curves should satisfy the condition defined by Eqn. (3.7). When $v = 0$ and $v = 1$ are assigned to Eqn. (3.7), and Eqn. (A.1) is obtained.

$$b_0 = k_0 a_0 + h_0 c_0, \quad b_3 = k_1 a_3 + h_1 c_2 \qquad (A.1)$$

Let a_0^3 be the vector between control points of Bezier boundary curve a_0 and b_0, a_3^3 be the vector between control points of Bezier boundary curve a_3 and b_3. Vectors a_1^3, a_2^3 are obtained by Eqn. (A.2).

$$a_0^3 = \frac{a_0 + b_0}{|a_0 + b_0|}, \quad a_1^3 = \frac{2a_0^3 + a_3^3}{3}, \quad a_2^3 = \frac{a_0^3 + 2a_3^3}{3},$$
$$a_3^3 = \frac{a_3 + b_3}{|a_3 + b_3|}. \qquad (A.2)$$

Here, to satisfy Eqn. (A.1), the scalar functions $k(v)$ and $h(v)$ about v are assumed to be linear functions. From Eqn. (3.7) and (3.8), the Eqn. (A.3) is obtained using the vectors between the control points of the surface (See Fig. 5(b)). Where, $B_i^3(v)$ is Bernstein base polynomial [1].

$$\sum_{i=0}^{3} B_i^3(v) b_i = \{k_0(1-v) + k_1 v\} \sum_{i=0}^{2} B_i^2(v) a_i^2$$
$$+ \{(1-v)h_0 + v h_1\} \sum_{i=0}^{2} B_i^2(v) c_i \qquad (A.3)$$

Since the left side of the Eqn. (A.3) is cubic, the degree of polynomial a_i^2 is limited to quadratic. Therefore, when we assume a_i^2 using Eqn. (A.3), a_i^2 is calculated using Eqn. (A.4).

$$a_0^2 = a_0^3, \quad a_1^2 = \frac{3a_1^3 - a_0^3}{2} = \frac{3a_2^3 - a_3^3}{2}, \quad a_2^2 = a_3^3. \qquad (A.4)$$

The control vectors b_1 and b_2 can be derived from Eqn. (3.7), (3.8) and (A.3).

$$b_1 = \frac{(k_1 - k_0)a_0^3}{3} + k_0 a_1^3 + \frac{2h_0 c_1}{3} + \frac{h_1 c_0}{3},$$
$$b_2 = k_1 a_2^3 - \frac{(k_1 - k_0)a_3^3}{3} + \frac{h_0 c_2}{3} + \frac{2h_1 c_1}{3}. \qquad (A.5)$$